Supplementary Information

A. Emissions
B. Model Performance Evaluation

A. Emissions

Table A1. Daily average SNAP sector emissions in August 2010.

SNAP Sector	Emissions (kg/day)					
	NO_x		$PM_{2.5}$		SO_2	
	Area sources	Point sources	Area sources	Point sources	Area sources	Point sources
SNAP 1: Energy	0	1201	0	8523	0	1535
SNAP 2: Residential Combustion	497	133	633	5223	464	60
SNAP 34: Industry*	0	428	0	10217	0	494
SNAP 5: Extraction and Distribution of Fossil Fuels	198	28	339	1484	814	56
SNAP 6: Solvent and Product use	5	0	744	0	6	0
SNAP 7: Road transport	161684	0	12935	0	3067	0
SNAP 8: Non-road transport	187226	0	26975	0	113166	0
SNAP 9: Waste treatment	11	8	55	1331	3	1
SNAP 10: Agriculture	936	0	16670	0	244	0

* Includes industrial combustion and industrial processes, previously SNAP sectors 3 and 4 respectively

Table A1. Daily average SNAP sector emissions in February 2010.

SNAP Sector	Emissions (kg/day)					
	NO_x		$PM_{2.5}$		SO_2	
	Area sources	**Point sources**	**Area sources**	**Point sources**	**Area sources**	**Point sources**
SNAP 1: Energy	0	1793	0	12739	0	2274
SNAP 2: Residential Combustion	3644	976	5960	49145	5148	663
SNAP 34: Industry*	0	579	0	14140	0	672
SNAP 5: Extraction and Distribution of Fossil Fuels	197	28	339	1482	813	56
SNAP 6: Solvent and Product use	4	0	644	0	5	0
SNAP 7: Road transport	147013	0	11815	0	2786	0
SNAP 8: Non-road transport	186988	0	26874	0	113394	0
SNAP 9: Waste treatment	11	8	55	1331	3	1
SNAP 10: Agriculture	138	0	2177	0	94	0

*Includes industrial combustion and industrial processes, previously SNAP sectors 3 and 4 respectively

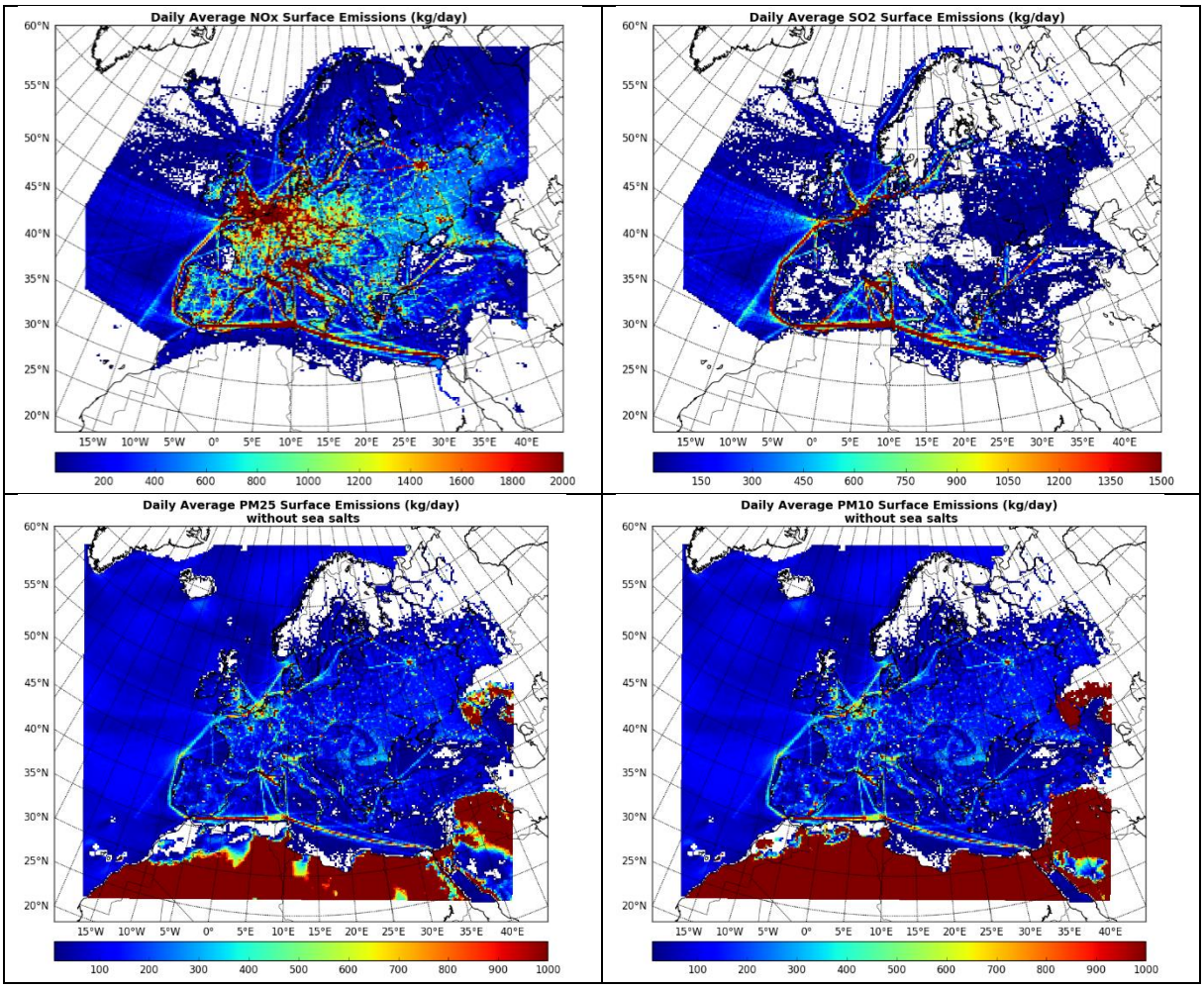

Figure A1. Daily average total NOx, SO_2, $PM_{2.5}$ and PM_{10} surface emissions in August 2010.

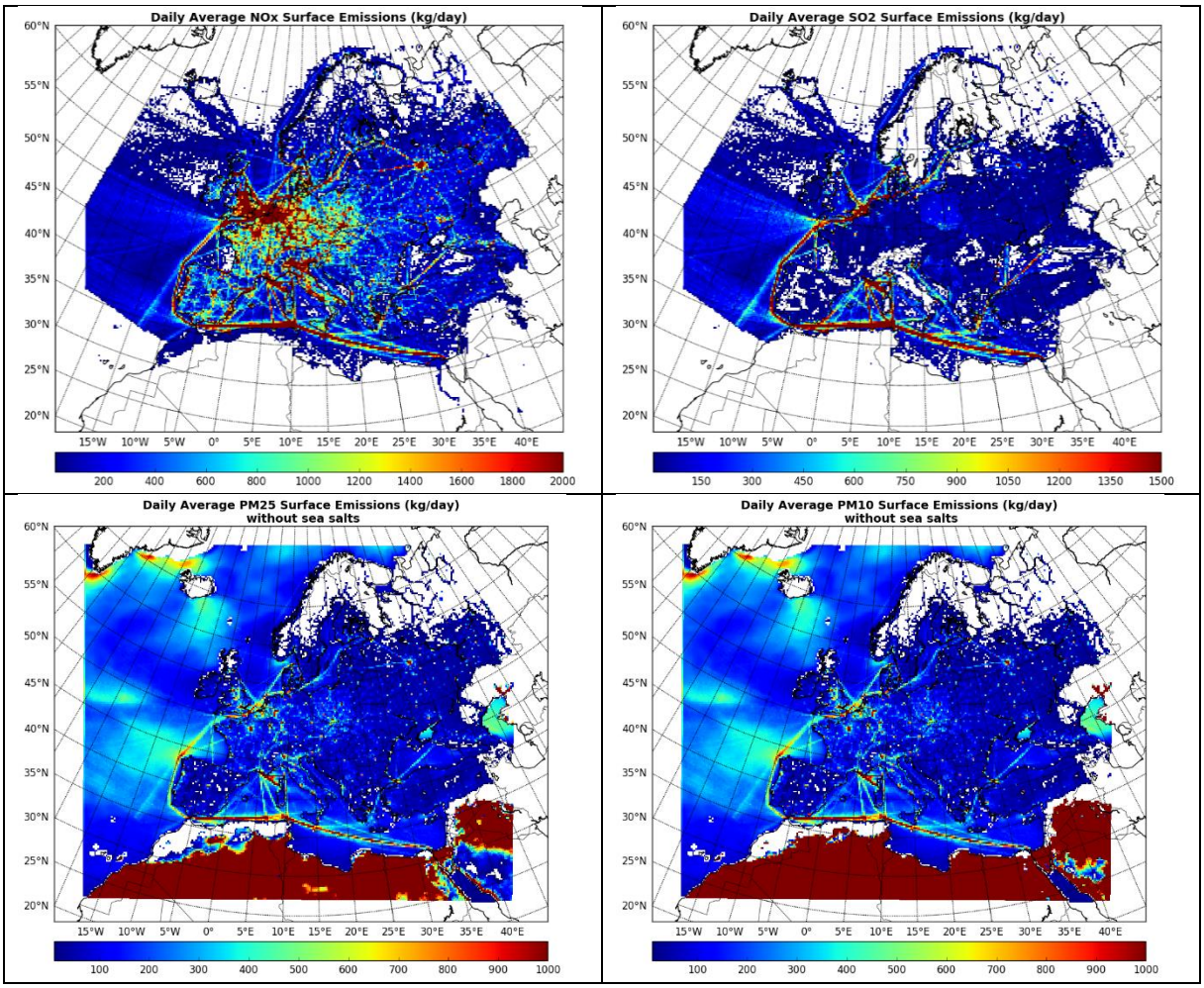

Figure A2. Daily average total NOx, SO_2, $PM_{2.5}$ and PM_{10} surface emissions in February 2010.

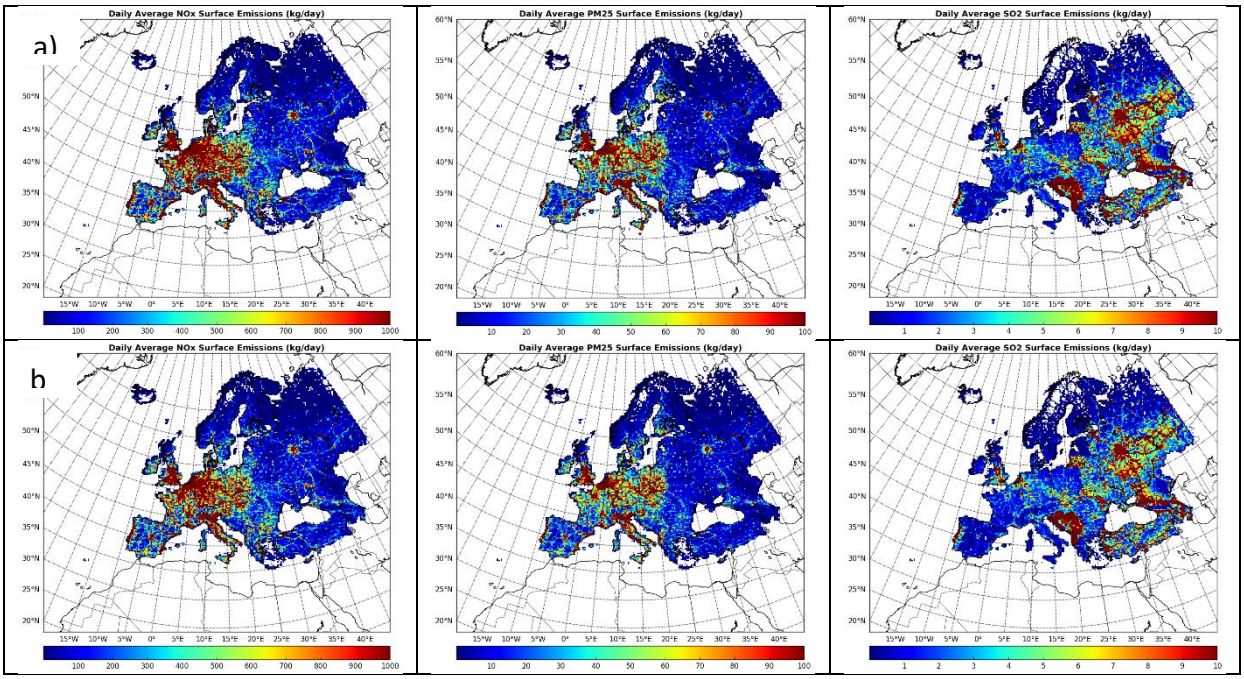

Figure A3. Daily average NOx, $PM_{2.5}$ and SO_2 surface emissions from SNAP Sector 7 (road transport) in a) August 2010 and b) February 2010.

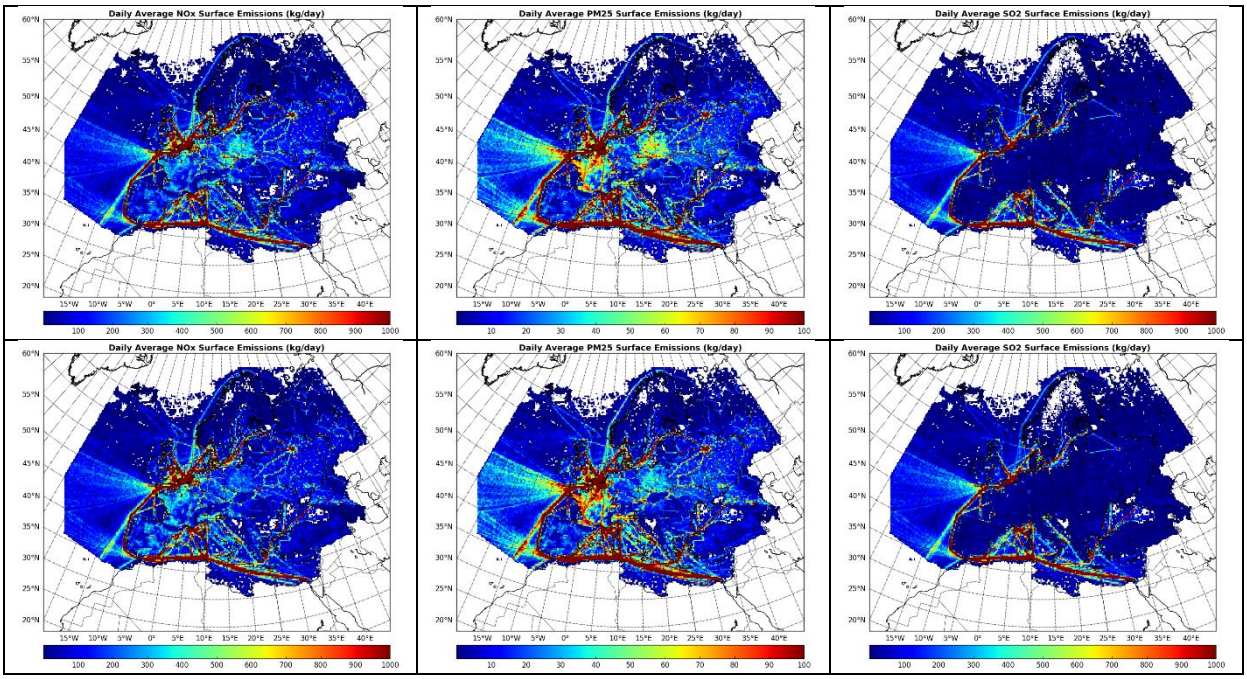

Figure A4. Daily average NOx, $PM_{2.5}$ and SO_2 surface emissions from SNAP Sector 8 (non-road transport) in a) August 2010 and b) February 2010.

a)

b)

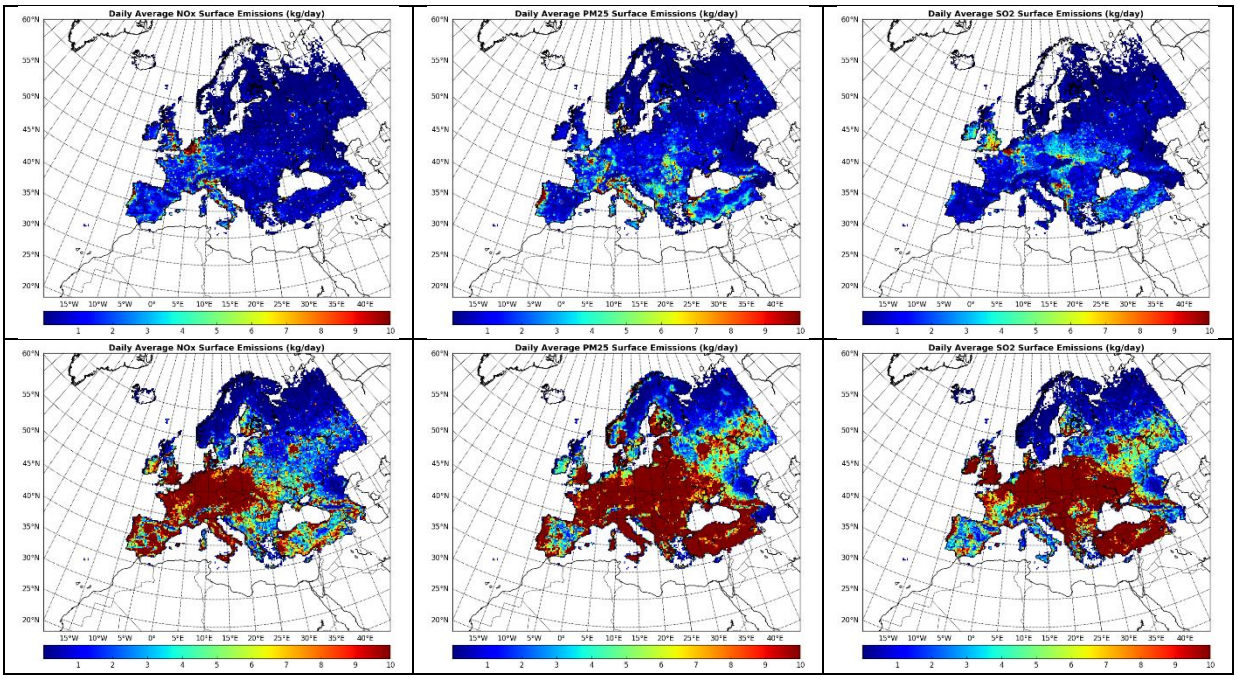

Figure A5. Daily average NOx, $PM_{2.5}$ and SO_2 surface emissions from SNAP Sector 2 (residential combustion) in a) August 2010 and b) February 2010.

B. Model Performance Evaluation

B1. Statistical indicators for model performance evaluation

The statistical indicators selected to evaluate the model performances have been defined as follows:

Normalized Mean Bias (NMB):

$$NMB = \frac{\frac{1}{N}\sum_{t=1}^{N}\left(C_{\mathrm{mod}}(x,t) - C_{obs}(x,t)\right)}{\frac{1}{N}\sum_{t=1}^{N} C_{obs}(x,t)} \qquad \text{(B.1)}$$

Normalized Mean Error (NME):

$$NME = \frac{\frac{1}{N}\sum_{t=1}^{N}\left|C_{\mathrm{mod}}(x,t) - C_{obs}(x,t)\right|}{\frac{1}{N}\sum_{t=1}^{N} C_{obs}(x,t)} \qquad \text{(B.2)}$$

Mean Fractional Bias (FB)

$$FB = \frac{1}{N}\sum_{t=1}^{N}\frac{C_{\mathrm{mod}}(x,t) - C_{obs}(x,t)}{(C_{obs}(x,t) + C_{\mathrm{mod}}(x,t))/2} \qquad \text{(B.3)}$$

Mean Fractional Error (FE)

$$FE = \frac{1}{N}\sum_{t=1}^{N}\frac{\left|C_{\mathrm{mod}}(x,t) - C_{obs}(x,t)\right|}{(C_{obs}(x,t) + C_{\mathrm{mod}}(x,t))/2} \qquad \text{(B.4)}$$

Correlation Index (r)

$$r = \frac{\sum_{t=1}^{N}\left(C_{\mathrm{mod}}(x,t)-\overline{C}_{\mathrm{mod}}(x)\right)\cdot\left(C_{obs}(x,t)-\overline{C}_{obs}(x)\right)}{\sqrt{\sum_{t=1}^{N}\left(C_{\mathrm{mod}}(x,t)-\overline{C}_{\mathrm{mod}}(x)\right)^2}\cdot\sqrt{\sum_{t=1}^{N}\left(C_{obs}(x,t)-\overline{C}_{obs}(x)\right)^2}} \qquad \text{(B.5)}$$

Index of Agreement (IA)

$$IA = 1 - \frac{\sum_{t=1}^{N}\left(C_{\mathrm{mod}}(x,t)-C_{obs}(x,t)\right)^2}{\sum_{t=1}^{N}\left(\left|C_{\mathrm{mod}}(x,t)-\overline{C}_{obs}(x)\right|+\left|C_{obs}(x,t)-\overline{C}_{obs}(x)\right|\right)^2} \qquad \text{(B.6)}$$

Root Mean Square Error (RMSE)

$$RMSE = \sqrt{\frac{1}{N}\sum_{t=1}^{N}\left(C_{\mathrm{mod}}(x,t)-C_{obs}(x,t)\right)^2} \qquad \text{(B.7)}$$

B2. Spatial performance evaluation

The spatial distribution of CAMx performance is reported in Figures B1 through B12 for both AB and RB sites.

SO_2 concentration is correctly reproduced in Central-Western Europe, while it is partially underestimated at Spanish sites and in the Po Valley. A more systematic underestimation is shown for Eastern Europe, that is characterized by the highest observed concentrations (yearly mean values greater than 4 ppb). SO_2 underestimation in Eastern Europe may imply a corresponding underestimation of the sulphate contribution to the total PM concentrations. When limiting the analysis to RB sites (Figure B2), we observe a better and more homogenous level of performance indicating that SO_2 underestimation in East EU is mostly related to urban sources.

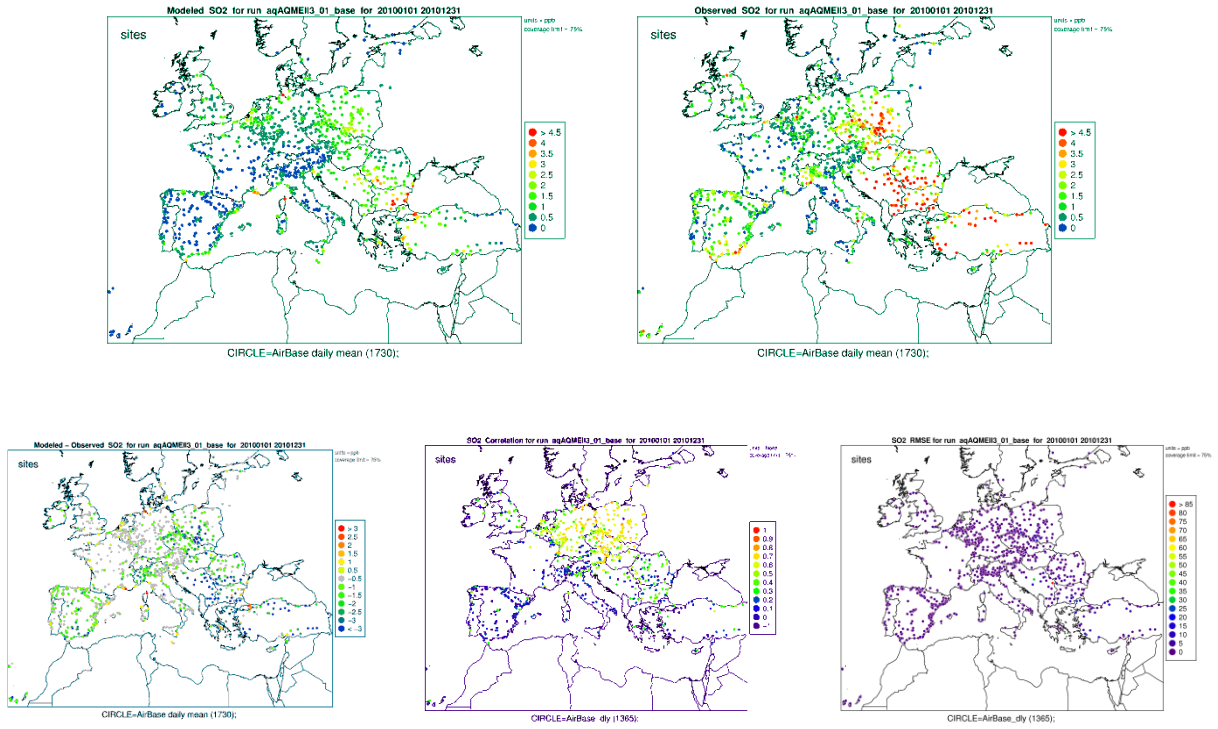

Figure B1 – Evaluation of CAMx performance for SO_2 at AB Airbase sites. Top panel: modelled and observed yearly mean concentrations. Bottom panel: yearly mean BIAS, Correlation and RMSE values computed for daily concentrations.

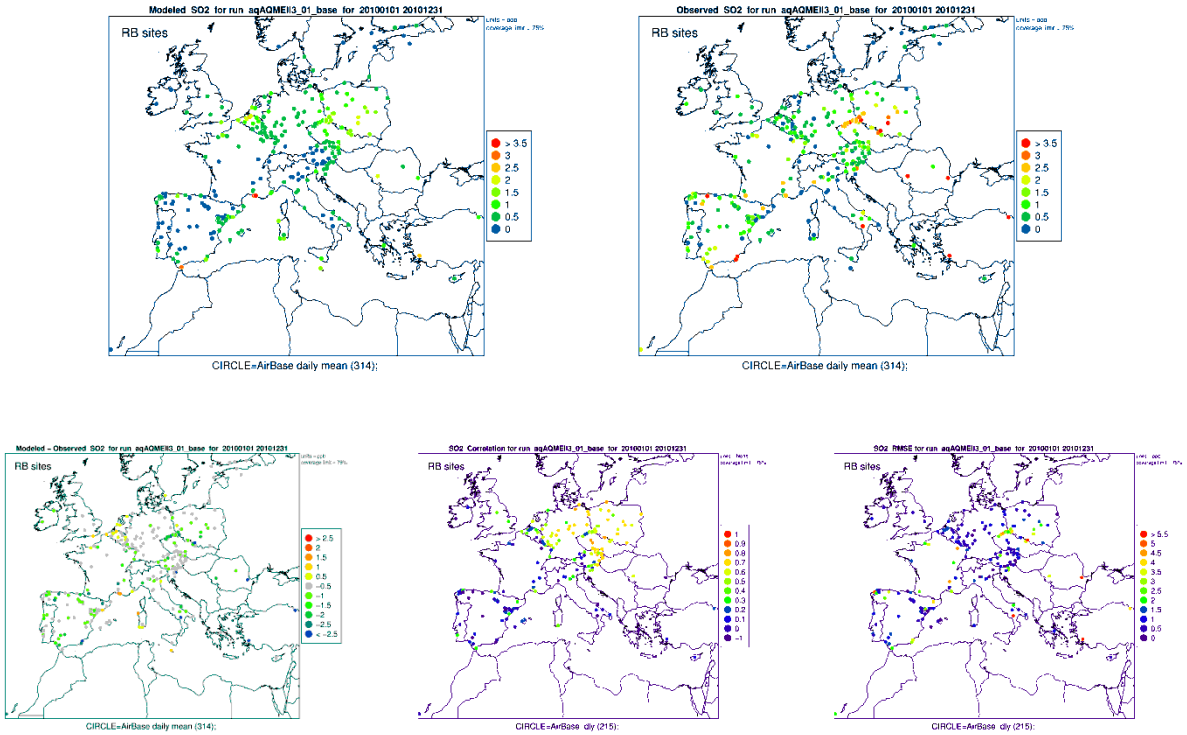

Figure B2 – Evaluation of CAMx performance for SO_2 at RB Airbase sites. Top panel: modelled and observed yearly mean concentrations. Bottom panel: yearly mean BIAS, Correlation and RMSE values computed for daily concentrations.

NO_2 performance is shown in Figures B3 and B4. NO_2 concentrations are generally underestimated but the mean BIAS is lower than 5 ppb at most of central and Western Europe sites. Higher underestimations are observed Italy and Eastern Europe. Correlation is higher than 0.5 at most of continental sites, while a more systematic decrease of model performance is observed along the coasts (e.g. Spain, Italy). This may suggest that evolution of the main sources at sea-land interface is not correctly reproduced. As expected, BIAS clearly decreases when moving to RB sites only, with yearly RMSE lower than 4-6 ppb at most sites. Conversely CAMs still shows a worsening in temporal correlation from in-land to coastal sites.

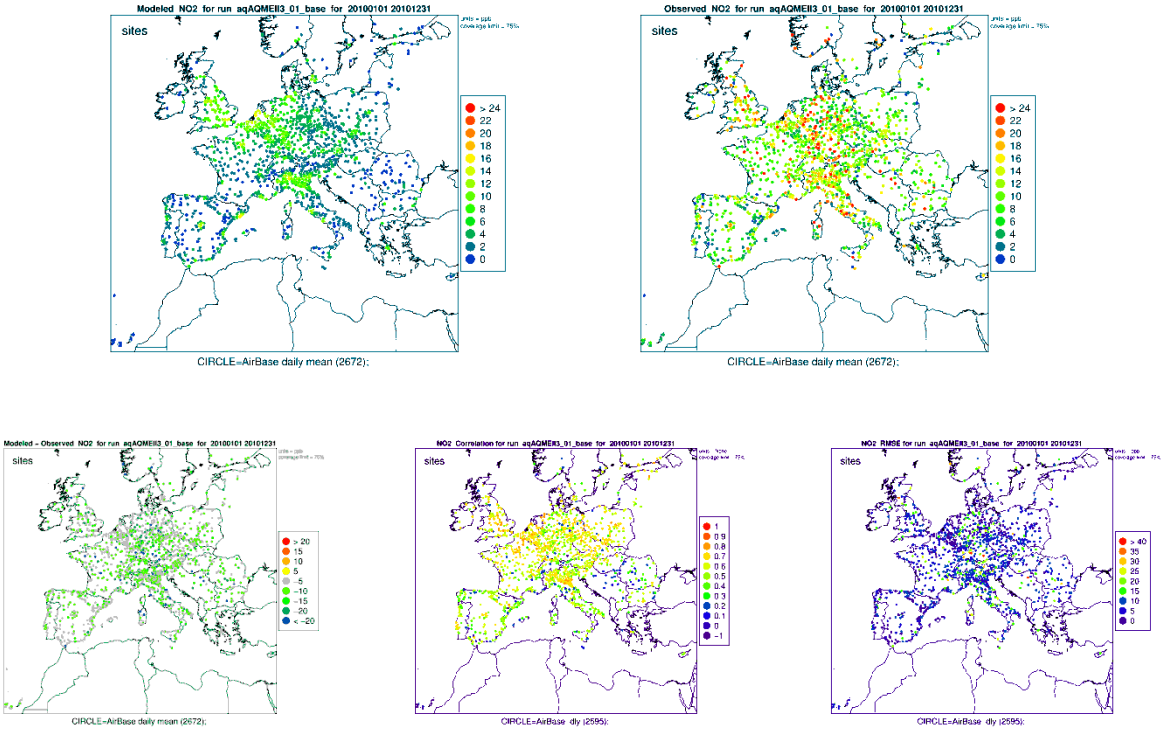

Figure B3 – Evaluation of CAMx performance for NO_2 at AB Airbase sites. Top panel: modelled and observed yearly mean concentrations. Bottom panel: yearly mean BIAS, Correlation and RMSE values computed for daily concentrations.

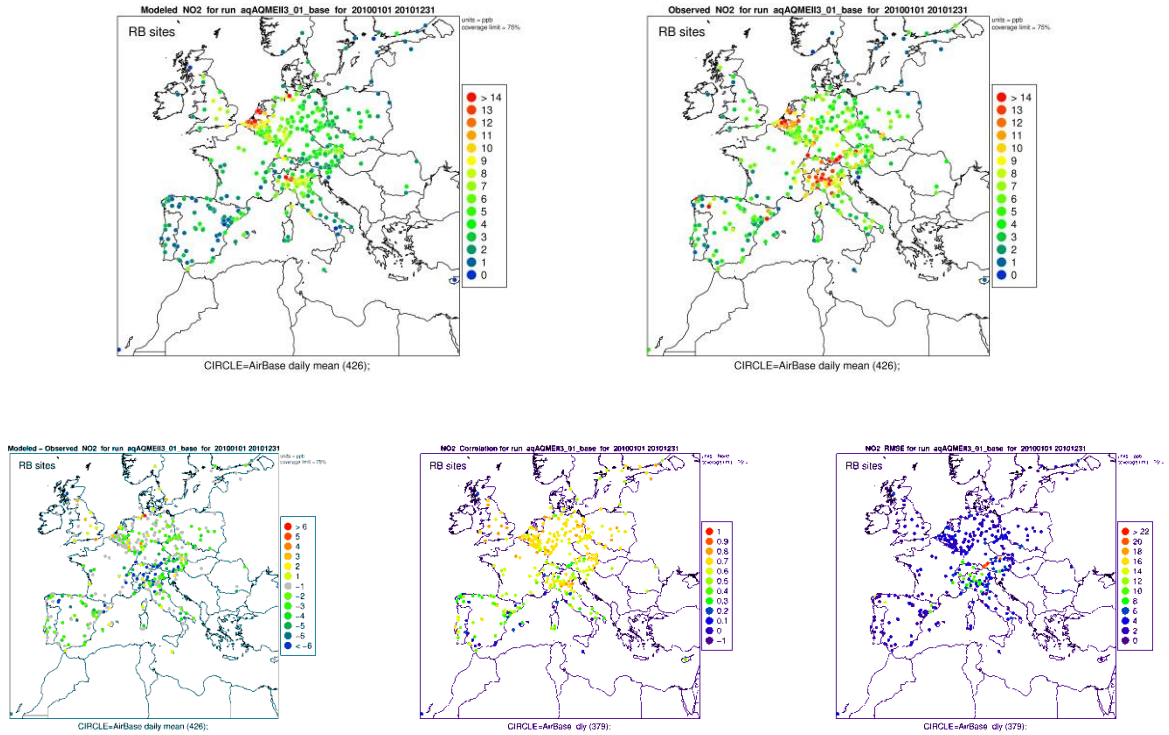

Figure B4 – Evaluation of CAMx performance for NO_2 at RB Airbase sites. Top panel: modelled and observed yearly mean concentrations. Bottom panel: yearly mean BIAS, Correlation and RMSE values computed for daily concentrations.

Ozone concentration shows a clear increasing gradient moving from NW to SE, stronger than the measured one. Indeed, observed concentrations are correctly reproduced over the whole Western and Central Europe, but overestimated in the Mediterranean areas.

Such a discrepancy is clearly shown in the map of the mean bias for both AB (Figure B5) and RB (Figure B6) sites. Considering both BIAS and RMSE it can be noted that strongest overestimations take place in Italy (particularly in the complex region surrounding the Po Valley) and in SE Europe. This result could be influenced by two different source of error: an excess of downward vertical transport over complex terrain regions (e.g. the Alps) and an overestimation of the ozone accumulation and transport within the marine boundary layer in the Mediterranean Sea.

Temporal correlation is very well reproduced over the whole domain (higher than 0.7), again with the exception of some coastal sites where correlation decreases to 0.5-0.4.

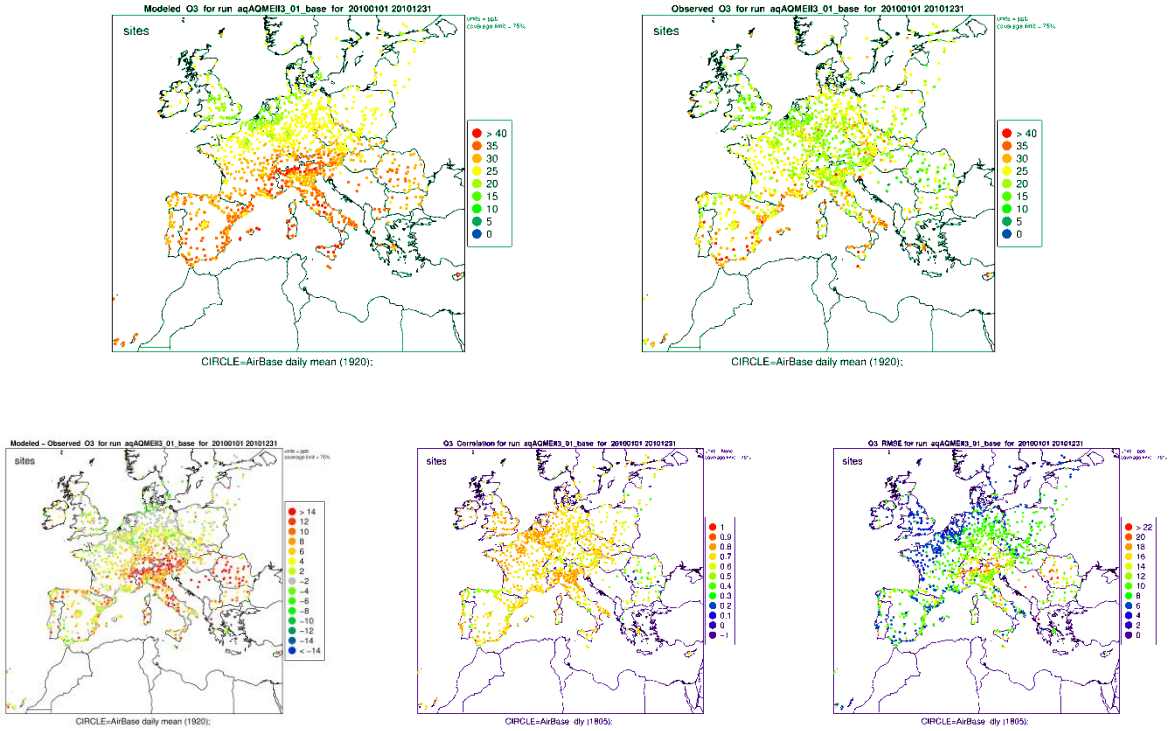

Figure B5 – Evaluation of CAMx performance for O_3 at AB Airbase sites. Top panel: modelled and observed yearly mean concentrations. Bottom panel: yearly mean BIAS, Correlation and RMSE values computed for daily concentrations.

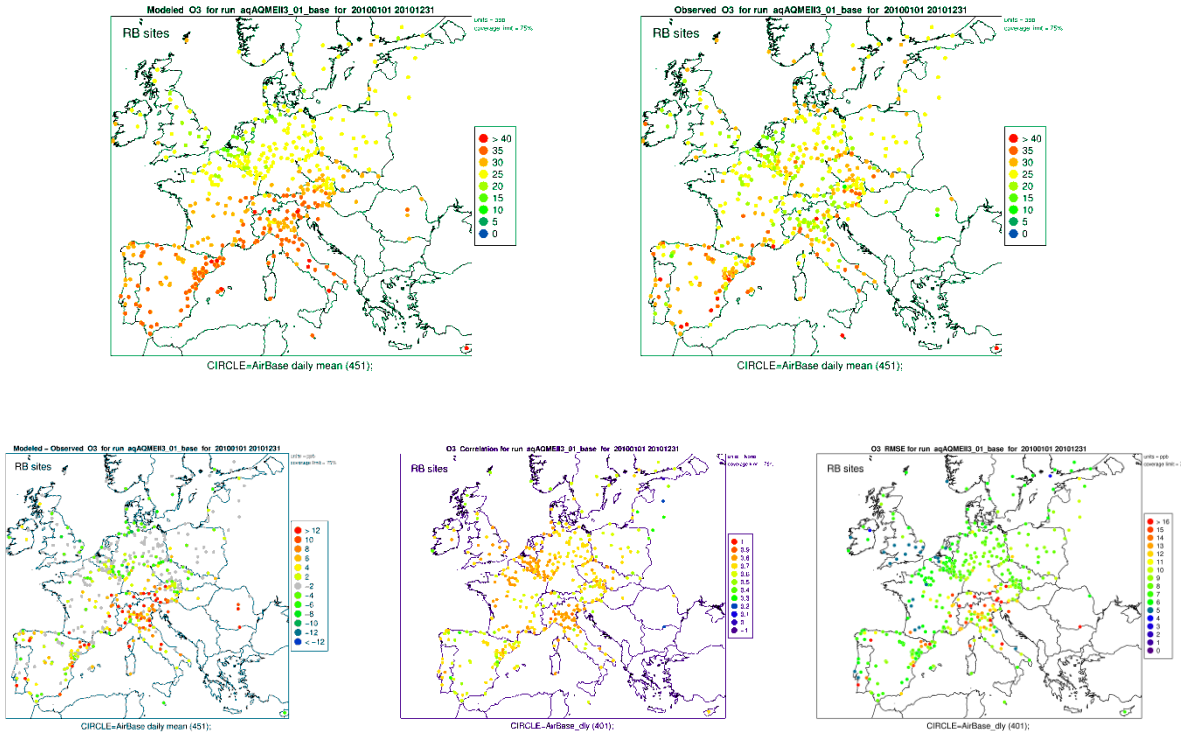

Figure B6 – Evaluation of CAMx performance for O_3 at RB Airbase sites. Top panel: modelled and observed yearly mean concentrations. Bottom panel: yearly mean BIAS, Correlation and RMSE values computed for daily concentrations.

The spatial pattern of O_X performance indicators (Figures B7 and B8) is similar to ozone, but with a clear reduction of the mean bias and RMSE values. Considering that O_X removes the effect of the local underestimation of NO_X titration, the spatial pattern of BIAS seems to confirm that there is an excess of ozone in the Mediterranean area.

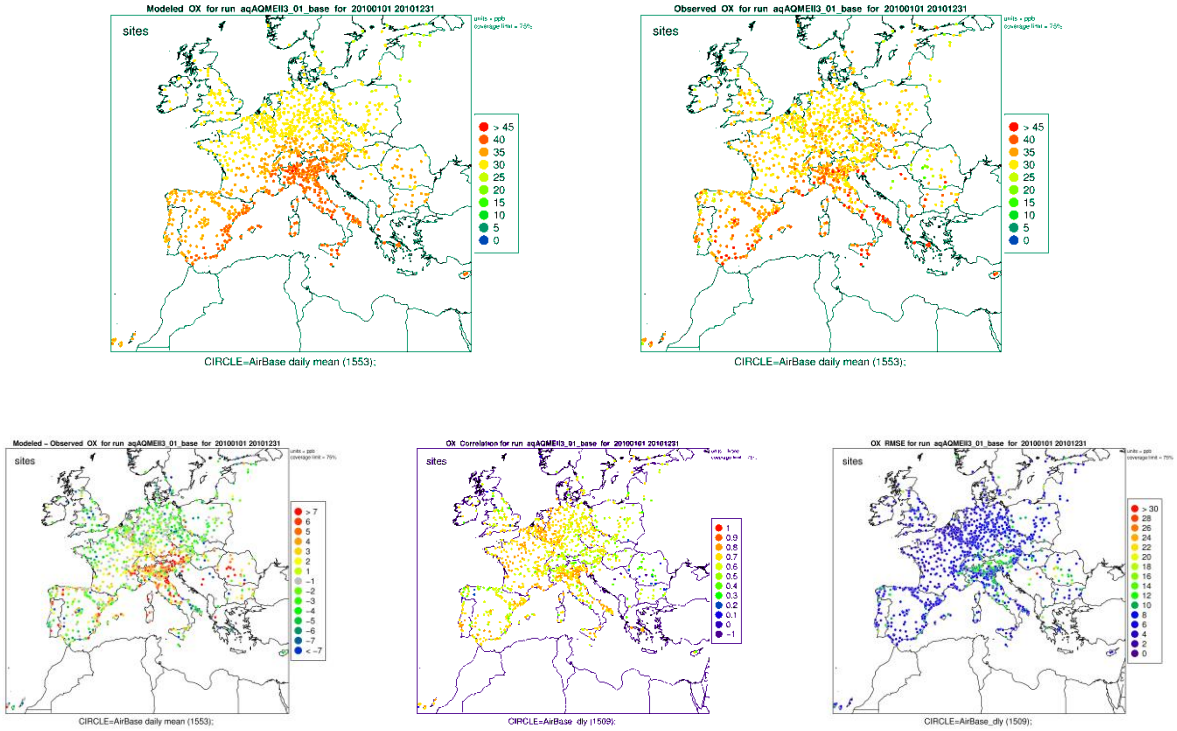

Figure B7 – Evaluation of CAMx performance for O_X at AB Airbase sites. Top panel: modelled and observed yearly mean concentrations. Bottom panel: yearly mean BIAS, Correlation and RMSE values computed for daily concentrations.

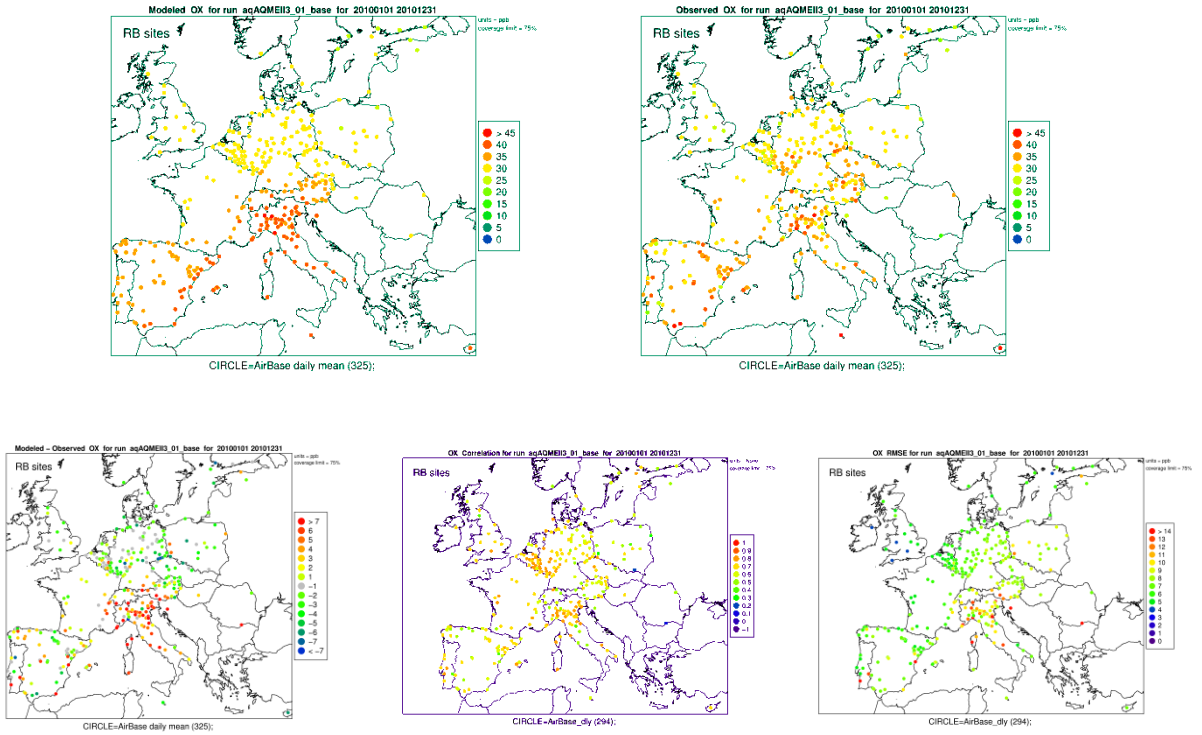

Figure B8 – Evaluation of CAMx performance for O_X at RB Airbase sites. Top panel: modelled and observed yearly mean concentrations. Bottom panel: yearly mean BIAS, Correlation and RMSE values computed for daily concentrations.

The spatial pattern of the PM_{10} performance indicators (Figure B9 and Figure B10) provide several interesting information. PM_{10} is correctly reproduced in a wide area of Western and Central Europe ranging from Spain to Western Poland (BIAS ranging between ± 5 $\mu g/m^3$). Differently, PM_{10} concentrations are systematically overestimated in UK and along the English Channel. These results could be related to a possible overestimation of sea salt contribution from Atlantic Ocean. This result seems confirmed also by the poor CAMx performance in reproducing temporal correlation over such area.

In Eastern and Mediterranean Europe PM_{10} concentrations are underestimated, as shown also in previous studies. PM_{10} underestimation in Eastern Europe are generally due to an underestimation of the strengths of the main sources influencing both primary compounds (e.g. Primary Organic Aerosol from biomass burning) and secondary species (e.g. Sulphate). PM_{10} underestimation in North and Central Italy, particularly in the Po Valley, are generally related to the underestimation of the strong stable conditions taking place during the cold season and giving rise to very severe PM episodes.

The results seem confirmed by the analysis of the RB subset, showing that PM_{10} concentrations are still overestimated in UK and close to the Channel, stating the probable influence of sea salt. Differently in Italy and Eastern EU, we can observe an increase in model performance, due to the weaker influence of urban sources at RB sites.

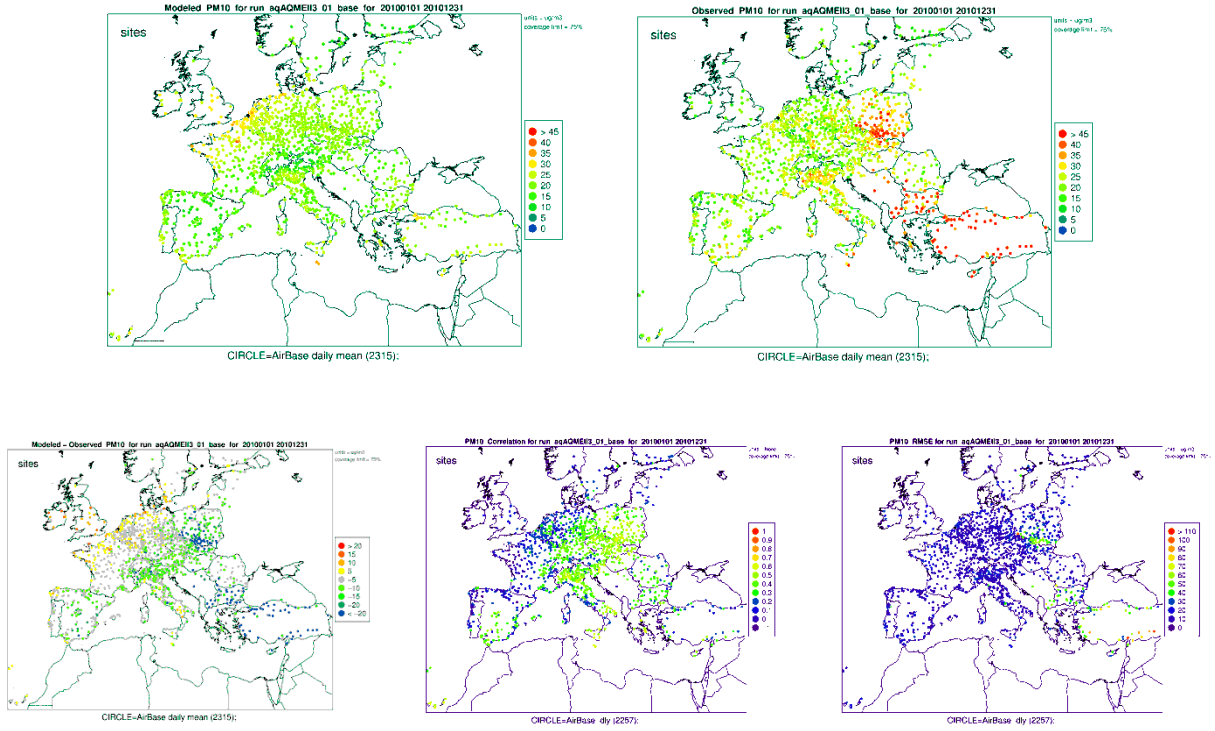

Figure B9 – Evaluation of CAMx performance for PM_{10} at AB Airbase sites. Top panel: modelled and observed yearly mean concentrations. Bottom panel: yearly mean BIAS, Correlation and RMSE values computed for daily concentrations.

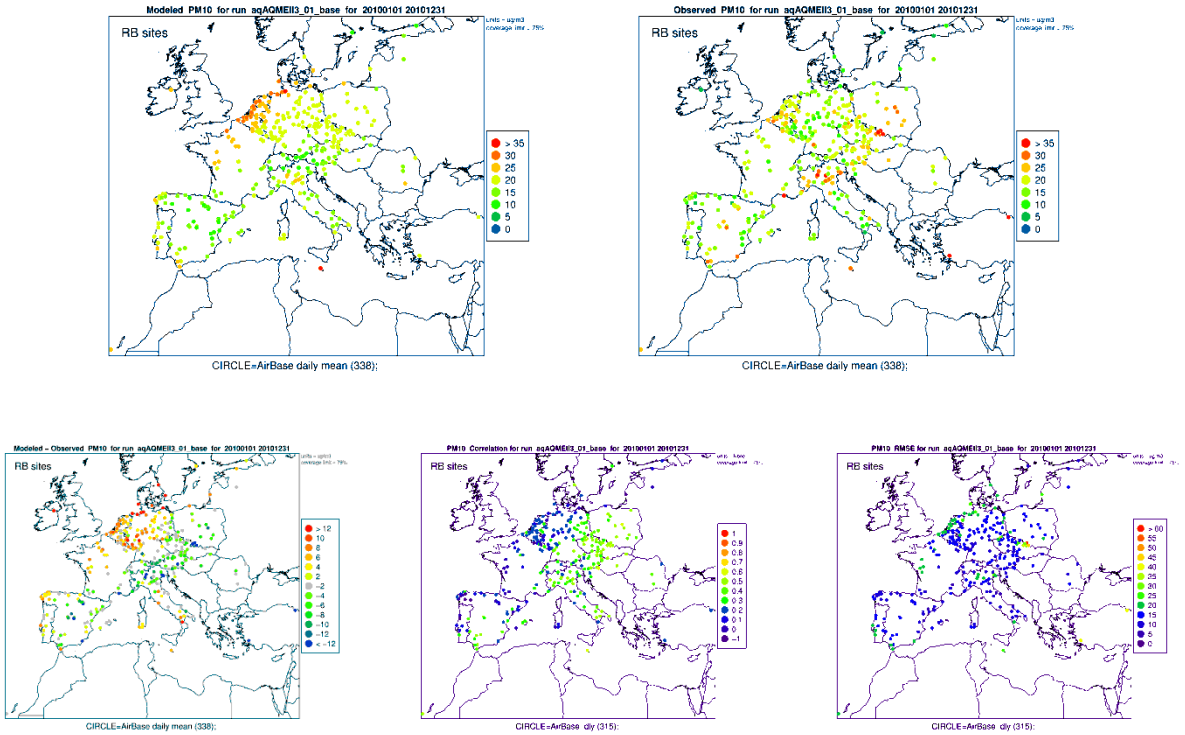

Figure B10 – Evaluation of CAMx performance for PM_{10} at RB Airbase sites. Top panel: modelled and observed yearly mean concentrations. Bottom panel: yearly mean BIAS, Correlation and RMSE values computed for daily concentrations.

An additional confirmation of the probable overestimation of the contribution of the natural sources to the PM coarse fraction can be derived from the analysis of $PM_{2.5}$ results (Figures B11 and B12). The PM fine fraction is better reproduced than PM_{10} over the whole Europe in terms of both mean BIAS and temporal correlation. This is particularly evident in Western Europe (UK, France, Benelux and Germany). Differently the model still underestimates observed concentrations in Italy and Eastern Europe, confirming that the model discrepancy is such regions is mostly related to anthropogenic sources. However, it is worth noting that the absolute values of the model bias for $PM_{2.5}$. is lower than PM_{10}, confirming that as a whole model performance for the PM fine fraction are more reliable than for PM_{10}.

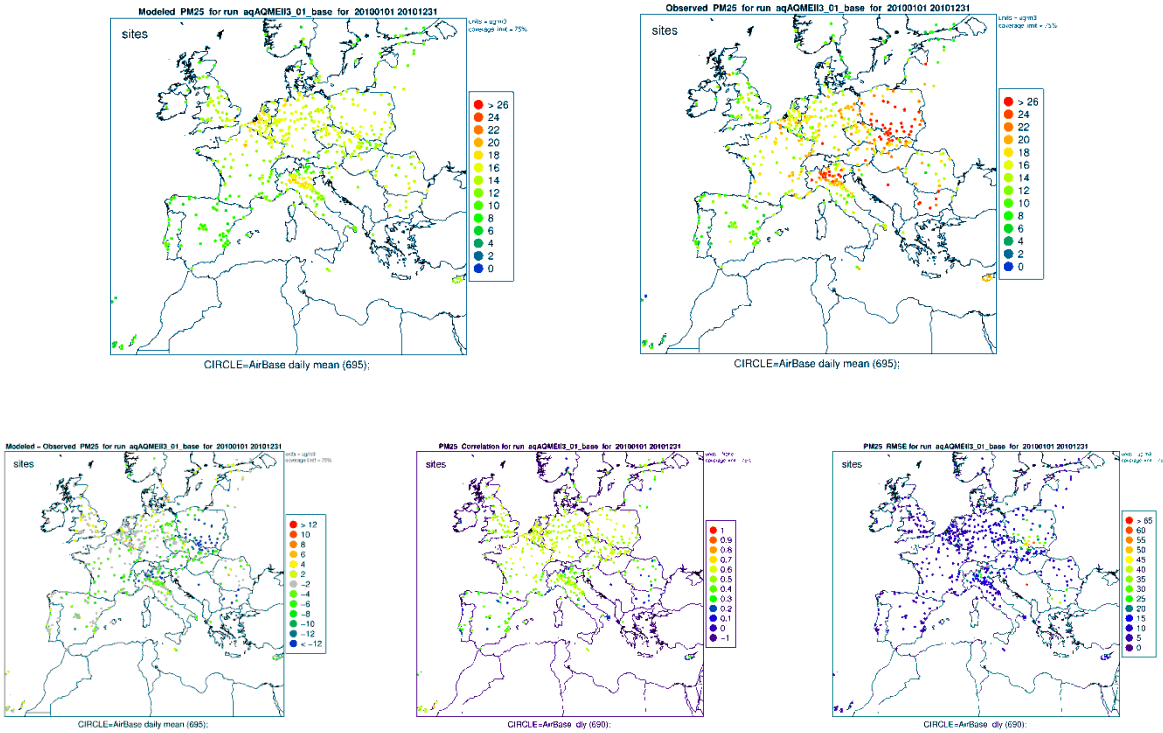

Figure B11 – Evaluation of CAMx performance for $PM_{2.5}$ at AB Airbase sites. Top panel: modelled and observed yearly mean concentrations. Bottom panel: yearly mean BIAS, Correlation and RMSE values computed for daily concentrations.

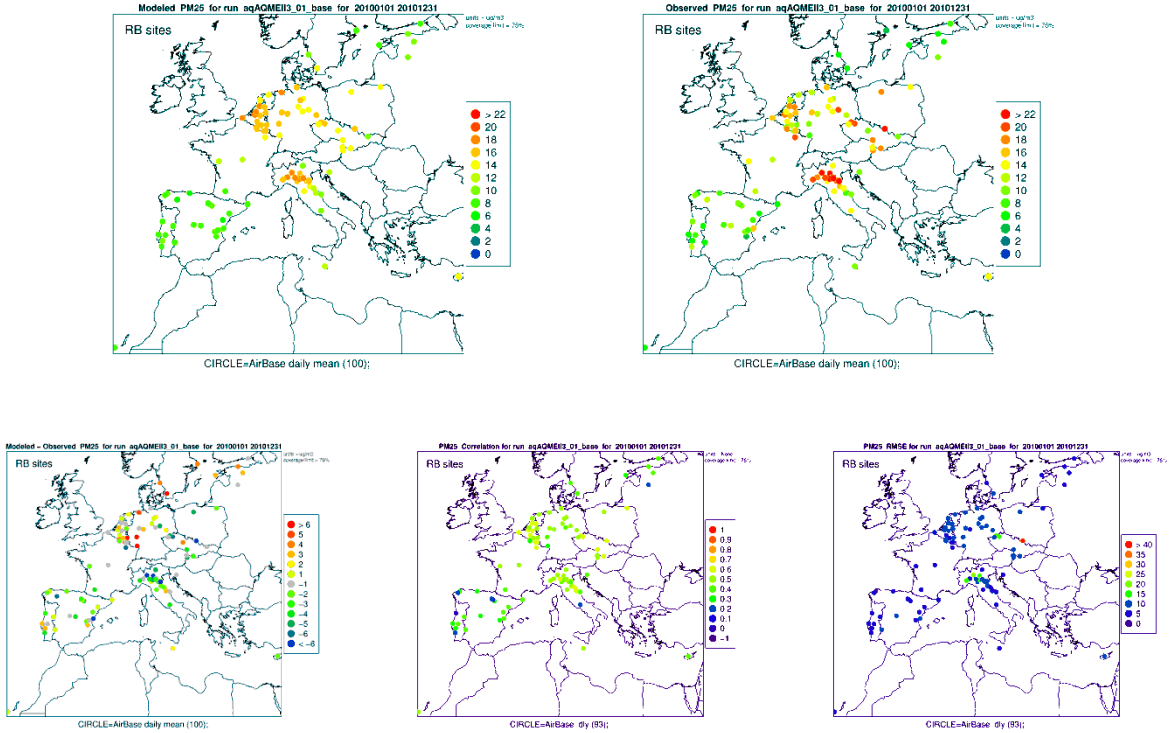

Figure B12 – Evaluation of CAMx performance for $PM_{2.5}$ at RB Airbase sites. Top panel: modelled and observed yearly mean concentrations. Bottom panel: yearly mean BIAS, Correlation and RMSE values computed for daily concentrations.

B2. Daily time series

The evaluation of model performance includes also the comparison of the temporal evolution of the daily mean concentration at AB (Figure B13) and RB (Figure B14) sites.

The analysis of the temporal time series confirm most of the previous findings, particularly the systematic underestimation of NO_2 concentration on the one side and the overestimation of the ozone daily mean on the other side. Differently, O_X concentration is very well reproduced: the model captures the long term seasonal cycle, as well as the different temporal variation taking place at a synoptic scale during the summer season. When moving to RB sites only, the very good performance for O_X is confirmed, but also the discrepancy for ozone and NO_2 is clearly reduced. Particularly at RB sites the all the main percentiles of the yearly distribution of the observed concentrations are slightly and uniformly overestimated by 2-3 ppb.

The model provides reasonable performance for PM_{10} concentration, partially due to an error compensation taking place late winter and during fall, where the model overestimates, and the summer season when the model underestimates. Limiting the analysis to the RB sites only we can observe a substantial improvement during summer, while the overestimation at the end and beginning of cold season are confirmed.

Finally, the analysis of the temporal evolution of CAMx results confirms the good model performance in reproducing the $PM_{2.5}$ daily mean concentrations. At AB sites the model correctly reproduces the seasonal evolution also capturing some episodes taking place in February and December. This is confirmed also by the analysis of the main percentiles at both AB and RB only sites.

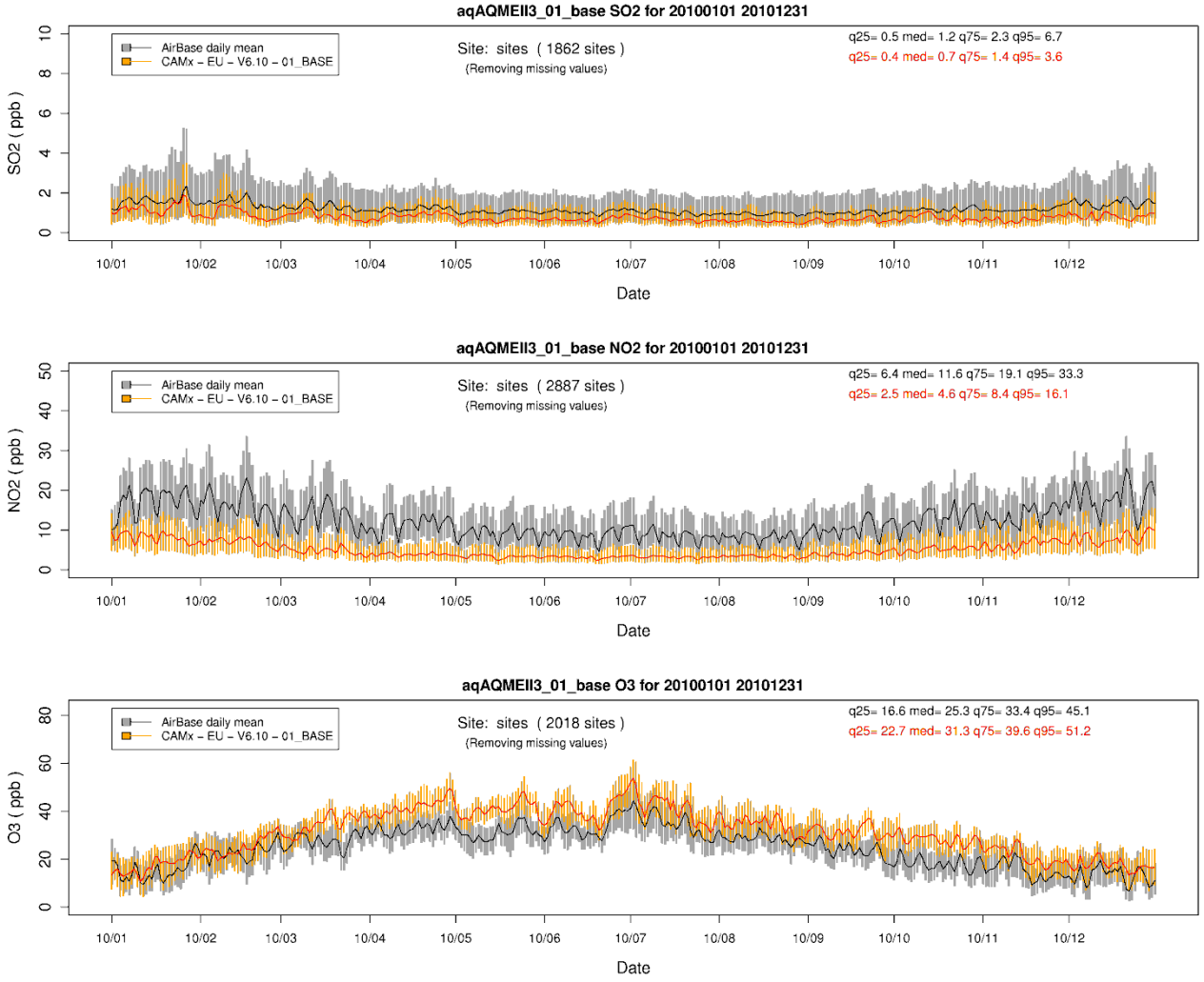

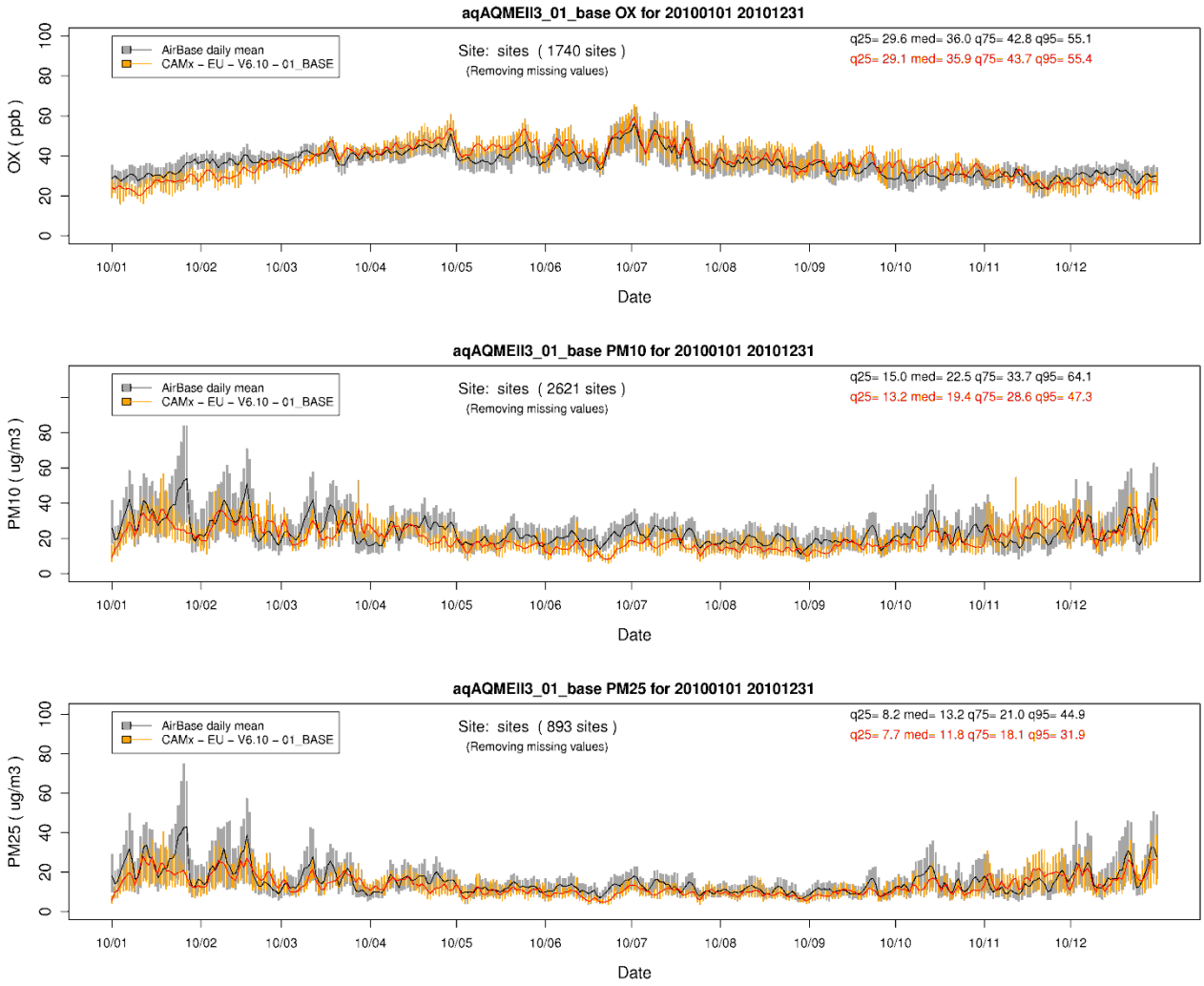

Figure B13 - Time series of the box and whisker plots for the distribution of the observed (black/grey) and computed (red/orange) daily concentrations of SO2, NO2, O3, OX (=O3+NO2), PM10 and PM2.5 at All Background (AB) Airbase sites. Bars show the interquartile range, lines the median values. Values for the 25th, 50th, 75th, and 95th quantiles of the whole yearly time series are reported too.

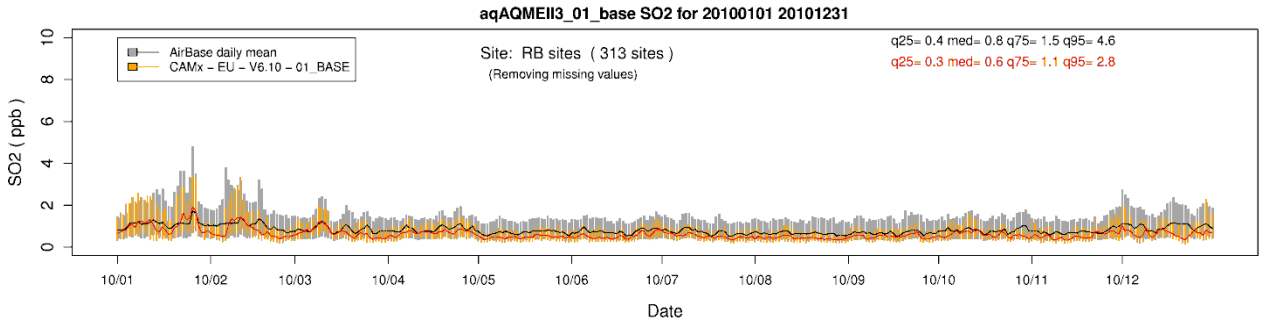

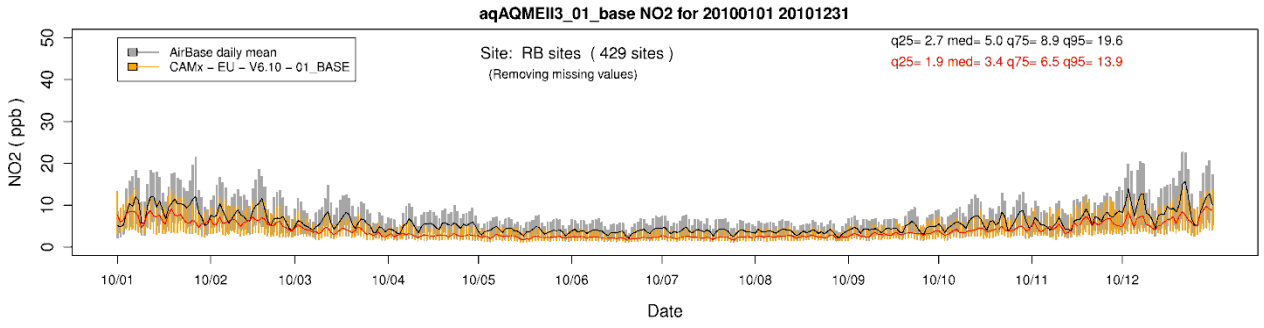
aqAQMEII3_01_base NO2 for 20100101 20101231
AirBase daily mean
CAMx – EU – V6.10 – 01_BASE
Site: RB sites (429 sites)
(Removing missing values)
q25= 2.7 med= 5.0 q75= 8.9 q95= 19.6
q25= 1.9 med= 3.4 q75= 6.5 q95= 13.9
NO2 (ppb)
0
10
20
30
40
50
10/01
10/02
10/03
10/04
10/05
10/06
10/07
10/08
10/09
10/10
10/11
10/12
Date

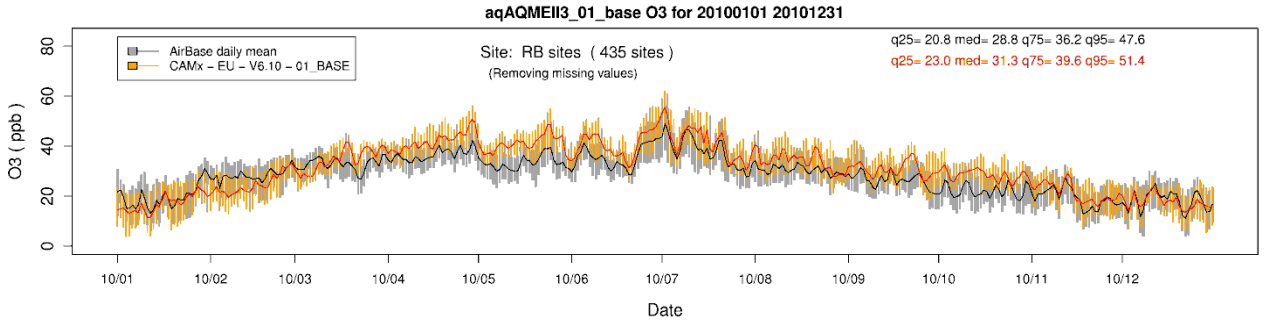
aqAQMEII3_01_base O3 for 20100101 20101231
AirBase daily mean
CAMx – EU – V6.10 – 01_BASE
Site: RB sites (435 sites)
(Removing missing values)
q25= 20.8 med= 28.8 q75= 36.2 q95= 47.6
q25= 23.0 med= 31.3 q75= 39.6 q95= 51.4
O3 (ppb)
0
20
40
60
80
10/01
10/02
10/03
10/04
10/05
10/06
10/07
10/08
10/09
10/10
10/11
10/12
Date

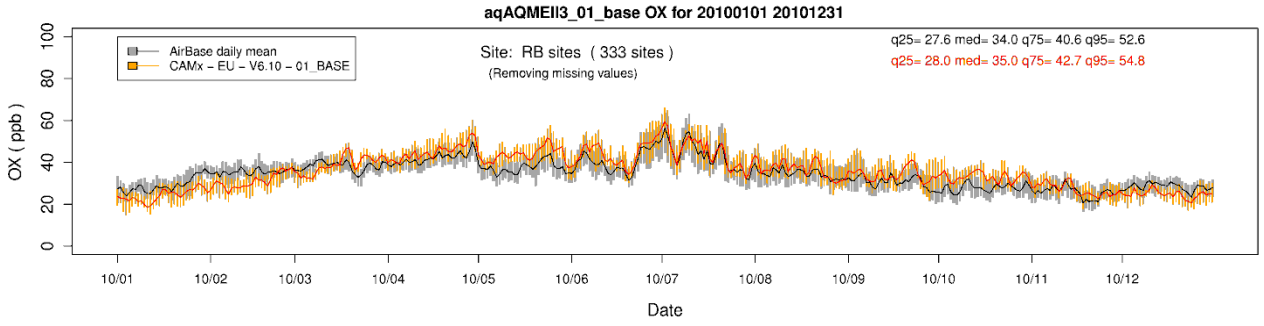
aqAQMEII3_01_base OX for 20100101 20101231
AirBase daily mean
CAMx – EU – V6.10 – 01_BASE
Site: RB sites (333 sites)
(Removing missing values)
q25= 27.6 med= 34.0 q75= 40.6 q95= 52.6
q25= 28.0 med= 35.0 q75= 42.7 q95= 54.8
OX (ppb)
0
20
40
60
80
100
10/01
10/02
10/03
10/04
10/05
10/06
10/07
10/08
10/09
10/10
10/11
10/12
Date

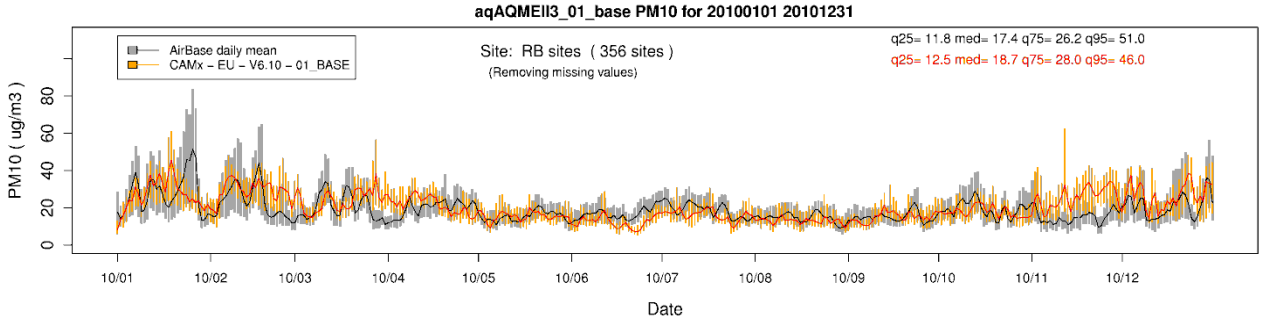
aqAQMEII3_01_base PM10 for 20100101 20101231
AirBase daily mean
CAMx – EU – V6.10 – 01_BASE
Site: RB sites (356 sites)
(Removing missing values)
q25= 11.8 med= 17.4 q75= 26.2 q95= 51.0
q25= 12.5 med= 18.7 q75= 28.0 q95= 46.0
PM10 (ug/m3)
0
20
40
60
80
10/01
10/02
10/03
10/04
10/05
10/06
10/07
10/08
10/09
10/10
10/11
10/12
Date

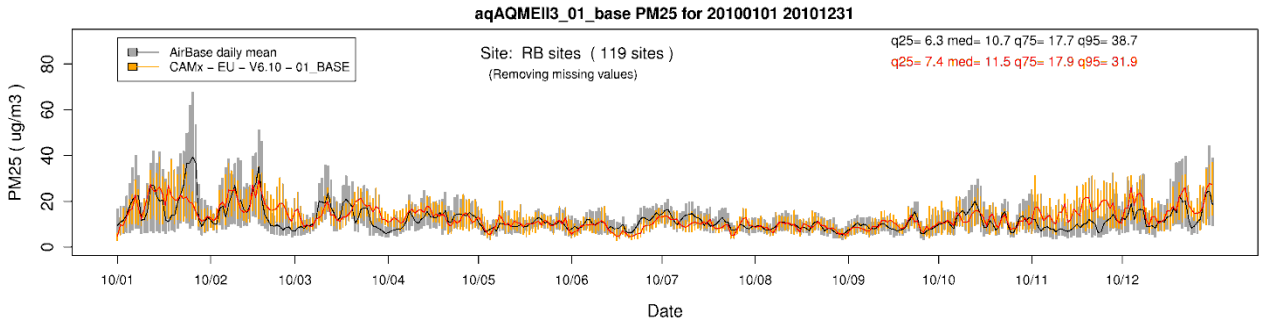

Figure B14 - Time series of the box and whisker plots for the distribution of the observed (black/grey) and computed (red/orange) daily concentrations of SO_2, NO_2, O_3, O_X (=O_3+NO_2), PM_{10} and $PM_{2.5}$ at All Background (AB) Airbase sites. Bars show the interquartile range, lines the median values. Values for the 25^{th}, 50^{th}, 75^{th}, and 95^{th} quantiles of the whole yearly time series are reported too.